AEM JOURNAL.ORG

Data Analysis of Textile-Based Sensors Based on AI Algorithm

Jianmin Chen
Huangshan Vocational Technical College, Huangshan 245000, Anhui, China
Corresponding author: Jianmin Chen (e-mail: 18055976138@163.com)

ABSTRACT Textile-based sensors have emerged as key components for wearable healthcare, intelligent sports analytics, and industrial monitoring, yet their practical deployment remains constrained by electromagnetic interference, motion artifacts, nonlinear multimodal coupling, and limited computational efficiency in dynamic environments. This study proposes a hybrid AI framework integrating CNN–Transformer architectures to address these challenges through adaptive wavelet denoising, GAN-based data augmentation, and attention-guided multimodal feature fusion for heterogeneous sensing signals. A lightweight deployment strategy combining model pruning and quantization reduces computational overhead by 70%, enabling real-time inference with latency below 50 ms on edge devices. Experimental validation demonstrates that the proposed framework achieves 95.3% motion recognition accuracy using an 8×8 pressure sensor array, attains an AUC of 0.95 for respiratory anomaly detection under low signal-to-noise conditions, and predicts fabric remaining useful life with an RMSE of 6.2 hours through physics-informed learning. By improving robustness against environmental disturbances and enhancing multimodal information extraction, the proposed method provides an effective computational solution for intelligent textile sensing systems and offers methodological support for electromagnetic interference mitigation, wearable sensing networks, and advanced smart sensing platforms involving wireless signal acquisition and integrated electromagnetic environments.

INDEX TERMS textile-based sensors, hybrid AI framework, multimodal fusion, electromagnetic interference mitigation, wearable sensing networks

I. INTRODUCTION

As an emerging intelligent sensing technology, textile-based sensors have shown great potential in various fields such as smart wearables, health monitoring, and motion detection due to their unique advantages of flexibility, lightweight, and wearability [1]. The global smart textiles market is estimated to expand at a compound annual growth rate (CAGR) of 25% from 2021 to 2031, crossing the value of US$23.82 Bn by the end of 2031 [2]. In the field of smart wearables, textile-based sensors can be perfectly integrated with clothing to monitor real-time physiological indicators of the human body, providing strong support for people's health management [3]. In terms of health monitoring, it can be used to monitor the physical condition of patients with chronic diseases, detect abnormal situations in a timely manner, and issue alerts [4]. In the field of motion detection, textile-based sensors can accurately capture athletes' movements and postures, providing scientific basis for sports training and rehabilitation [5]. In recent years, the rapid development of flexible electronic technology and intelligent textiles has driven revolutionary applications of textile-based sensors in fields such as medical health [6], sports science [7], and industrial monitoring [8]. Compared with traditional rigid sensors, textile-based sensors, with their high flexibility, stretchability, and seamless adhesion to the surface of the human body/object, can collect multimodal data in real time such as physiological signals (such as electrocardiogram [9], respiration [10], electromyography [11]), and motion posture [12] (pressure distribution, joint angle). However, the widespread application of textile-based sensors still faces two major bottlenecks. At the hardware level, sensors are susceptible to noise interference in dynamic environments such as human movement and temperature changes, leading to signal distortion [13]. At the data level, the nonlinear coupling characteristics of multimodal signals (resistance, capacitance, optical signals) make it difficult for traditional analysis methods to achieve high-precision feature extraction and pattern recognition [14]. Although researchers have attempted to optimize the data analysis process through various means, the following issues have not been effectively addressed:

(1) High noise and signal drift [15]

Textile-based sensors are susceptible to environmental interference (such as electromagnetic noise, temperature and humidity changes) and motion artifacts (such as human body shaking) in practical applications. Although Wavelet

Transform [16] and Kalman Filter [17] are widely used for noise reduction, their parameters require manual tuning and are difficult to adapt to dynamically changing signal characteristics.

(2) Difficulty in multimodal data fusion [18]

Modern textile-based sensors often integrate multiple sensing units (such as pressure, temperature, humidity), but there are significant differences in the spatiotemporal resolution and physical dimensions of different modal data. For example, motion posture recognition requires simultaneous processing of high- frequency pressure signals (kHz-level) and low-frequency temperature signals (Hz-level). Traditional methods such as principal component analysis (PCA) [19] ignore temporal dependencies, resulting in low feature fusion efficiency.

(3) Insufficient generalization ability of the model

Although existing deep learning models, such as CNN and LSTM, perform well in laboratory environments, they are susceptible to individual differences (such as body shape and exercise habits) and sensor aging in real-world scenarios [20].

In response to the above challenges, this article proposes an "end-to-end AI driven textile-based sensors data analysis framework", with core objectives including:

Enhancing noise robustness: reducing the impact of environmental interference on the model through adaptive wavelet denoising and generative adversarial network (GAN) data augmentation [21];

Multimodal feature fusion: Design a hybrid neural network (CNN– Transformer) based on attention mechanism to achieve dynamic weighted fusion of spatiotemporal features;

Lightweight and adaptive deployment: Combining model pruning with online incremental learning to enhance the real-time performance and scene adaptability of algorithms on edge devices such as smart bracelets and embedded terminals.

II. LITERATURE REVIEW

A. PROGRESS IN TEXTILE-BASED SENSORS TECHNOLOGY

Textile-based sensors technology has made significant progress in recent years and has become an important research direction in the fields of intelligent wearable devices and electronic textiles. From a global perspective, the research content of domestic and foreign scholars in this field covers multiple aspects such as material innovation [22], sensing mechanisms [23], application expansion [24], and future development directions [25]. Recent research has focused on creating highly sensitive and multifunctional textile-based sensors that can operate effectively in diverse environments. For instance, Chen et al. [26] developed a pressure sensor utilizing a hierarchical conductive fabric structure, which demonstrated remarkable sensitivity (15.78 kPa-1) and a wide detection range from 30 Pa to 700 kPa. This sensor's design allows for large-scale production and has potential applications in wearable human-machine interfaces (WHMIs) and robotics. Similarly, Zhou et al. [27] introduced a polyaniline-coated cotton knitted fabric that serves as a flexible strain sensor. This sensor exhibited a significant reduction in resistivity and a maximum gauge factor exceeding 30, making it suitable for monitoring human activities and physical signs. These innovations underscore the trend towards integrating advanced materials into textile-based sensors to enhance their performance. The development of capacitive sensors has also seen significant progress. Ye et al. [28] presented an all-fabric capacitive sensor capable of detecting pressure and enabling non-contact instructions. This sensor achieved a pressure-sensing sensitivity of 0.38 kPa-1 and demonstrated excellent cycling stability, making it ideal for applications in healthcare monitoring and human-computer interfaces. Moreover, the exploration of electrochemical sensors has led to the creation of wearable devices that can monitor sweat metabolites. Zhang et al. [29] proposed a dual-function flexible wearable sweat electrochemical sensor that utilizes Janus fabric for efficient sweat collection and detection of various components, including sodium and glucose. This sensor's design allows for real-time monitoring, showcasing the potential for non-invasive health assessments.

B. APPLICATION OF AI ALGORITHMS IN FABRIC DATA ANALYSIS

In recent years, significant progress has been made in the application of artificial intelligence (AI) algorithms in fabric data analysis, bringing revolutionary changes to the textile industry. From fabric defect detection to performance prediction, and then to design optimization, AI technology is gradually penetrating into every aspect of textile production, promoting the intelligent and efficient development of the industry. AI algorithms have demonstrated powerful capabilities in fabric defect detection. For example, support vector machine (SVM) is used to classify common fabric defects such as wrinkling, breakage, and oil stains, with high classification accuracy [30]. In addition, the application of Convolutional Neural Networks (CNNs) in the field of image processing has made breakthrough progress [31], which can automatically detect and classify fabric defects, such as porosity calculation, fabric pattern recognition, etc. These technologies not only improve detection efficiency, but also reduce manual inspection errors and costs. In terms of predicting fabric performance, artificial neural networks (ANN) and deep learning models are widely used to predict the mechanical properties, hand feel, and drape of fabrics. For example, BP neural networks are used to predict the heat transfer performance [32].

III. METHODS

A. DATA PREPROCESSING

The raw data of textile-based sensors usually contains high-frequency noise, baseline drift, and device drift, and signal normalization needs to be achieved through the following steps:

1) Noise Suppression and Signal Calibration

(1) Adaptive wavelet denoising

Using an improved threshold function (such as a semi soft threshold) to perform multi-scale decomposition on the signal, dynamically adjusting the wavelet basis (Daubechies-5) and decomposition layers (5-8 layers), the formula is as follows:

$$\hat{s}(t) = \sum_{j=1}^{N} \text{Threshold}\left(W_j(t), \lambda_j\right), \tag{1}$$

where $W_j(t)$ is the wavelet coefficient of the layer, j is the adaptive threshold, $\lambda_j = \sigma_j\sqrt{2\ln N}$, and σ_j is the standard deviation of noise in each layer. To justify the threshold selection, we evaluated hard, soft, and semi-soft threshold functions on EMG signals

(1 kHz sampling, 50 Hz powerline noise). The semi-soft threshold achieved superior PSNR (28.6 dB $\pm$ 1.2) versus hard (25.3 dB) and soft (26.8 dB) thresholds, balancing noise suppression and signal fidelity. Daubechies-5 basis was selected over Symlet-4 due to its 12% higher PSNR in low-SNR (< 10dB) conditions, validated on 5,000 EMG epochs.

(2) Temperature drift compensation

Based on the temperature resistance characteristic curve of the sensor, a polynomial regression model is constructed to correct signal offset in real-time.

$$R_{\text{corrected}} = R_{\text{raw}} - \sum_{k=0}^{3} a_k T^k, \tag{2}$$

where T is the temperature sensor reading, and the coefficient a_k is obtained through offline calibration.

2) Data Augmentation and Imbalance Handling

GAN Generative Adversarial Network: Design condition generators and discriminators to generate high fidelity synthetic data with a small amount of real data (such as abnormal respiratory waveforms). The generator structure is a 5-layer deconvolution network, with the input being the concatenation of noise vector z and category label y.

Temporal data augmentation: Apply random scaling ($\pm$ 10%), time distortion (window stretching/compression), and Gaussian jitter (SNR > 20 dB) to the original signal to enhance the model's robustness to dynamic changes.

B. FEATURE EXTRACTION AND FUSION

1) Manual Feature Engineering

Time domain features: mean, variance, zero crossing rate, Hjorth parameters (activity, mobility, complexity).

Frequency domain features: Fast Fourier Transform (FFT) energy spectrum, wavelet packet energy entropy (divided into 8 subbands).

Time–frequency joint feature: Extracting Mel frequency cepstral coefficients (MFCC) through short-time Fourier transform (STFT), suitable for speech signals (such as cough detection).

2) Automatic Extraction of Deep Features

Spatial feature extraction (CNN module): Design one-dimensional convolutional layers (Kernel size=5, Stride=2) and max pooling layers to capture local spatial patterns of sensor signals. For example, the two- dimensional topology of a pressure sensor array is converted into a channel dimension feature map through 1D-CNN.

Temporal dependency modeling (LSTM module): The bidirectional LSTM layer (Hidden units=128) captures long and short-term temporal dependencies and outputs a sequence of hidden states H = {h1, h2, . . . , hT}.

3) Multimodal Feature Fusion

Attention based dynamic weighting: After extracting features from multimodal data such as pressure, temperature, and resistance, a multi-head attention mechanism is introduced to calculate cross-modal correlation weights.

$$\text{Attention}(Q, K, V) = \text{Softmax}\left(\frac{QK^T}{\sqrt{d_k}}\right)V, \tag{3}$$

where Q, K, and V are the query, key, and value matrices mapped for different modal features, and d_k is the dimension scaling factor.

Feature cascading and dimensionality reduction: The weighted feature vectors are concatenated and compressed into a low dimensional space (such as 256 dimensions) through a fully connected layer (FC layer) to reduce redundant information.

C. MODEL ARCHITECTURE DESIGN

Design objectives for the hybrid CNN–Transformer architecture are: (1) recall $\geq$ 93.7% in cross-user scenarios after 10% fine-tuning; (2) real-time inference latency < 50 ms after 70% model compression; and (3) AUC = 0.97 at SNR = 5 dB for anomaly detection.

1) Hybrid Neural Network Framework (CNN–Transformer)

Input layer: preprocessed multimodal time series of shape (N, T, C), where N is the number of samples, T the number of time steps, and C the number of channels.

Feature extraction module: CNN branch: 3-layer one-dimensional convolution (Filters=64, 128, 256) extracts local features and outputs feature maps $F_{\text{CNN}} \in \mathbb{R}^{T\times 256}$.

Transformer branch: Positional encoding injects temporal information, and a 4-layer Transformer encoder (heads=8, feed forward dim=512) models global dependencies and outputs sequences $F_{\text{Trans}} \in \mathbb{R}^{T\times 512}$.

Feature fusion module: features are concatenated along the channel dimension and dynamically adjusted through a Gated Linear Unit (GLU) mechanism.

$$F_{\text{fusion}} = \sigma\left(W_g[F_{\text{CNN}}; F_{\text{Trans}}]\right) \odot \left(W_f[F_{\text{CNN}}; F_{\text{Trans}}]\right), \tag{4}$$

where σ is the Sigmoid function and W_g, W_f are the learnable parameters.

Output layer: classification task: fully connected layer + softmax output probability distribution; regression task: fully connected layer + linear activation, predict target values (such as remaining useful life). The architecture of the CNN–Transformer model is shown in Figure 1.

2) Lightweight Deployment Strategy

Quantization-aware training (QAT): Convert 32-bit floating-point parameters to 8-bit integers (INT8) while reducing accuracy loss through quantization error compensation algorithm (QEC).

Embedded inference optimization: Use TensorRT engine to perform layer fusion and kernel automatic tuning on the model and achieve real-time inference (latency < 50 ms) on NVIDIA Jetson Nano. Memory profiling on NVIDIA Jetson Nano (4 GB RAM) showed the compressed model reduced RAM usage from 2.7 GB (original FP32) to 0.8 GB (INT8), achieving proportional 70% reduction matching the pruning rate. The CNN branch consumed 0.3 GB (vs. 1.1 GB originally) due to filter pruning, while Transformer attention layers used 0.4 GB (vs. 1.3 GB) after head pruning.

D. PERFORMANCE EVALUATION INDICATORS

1) Classification Task Evaluation

Accuracy: Overall classification accuracy, suitable for category balanced scenarios. (Criteria: High: $\geq$ 90%)

F1 Score: The harmonic average of precision and recall, aimed at addressing class imbalance issues (such as anomaly detection). (Criteria: Medical anomaly detection: Target F1 > 0.85)

ROC-AUC: Evaluating the model's ability to distinguish between positive and negative samples based on the area under the subject's working characteristic curve. (Criteria: Excellent: $\geq$ 0.9)

2) Regression Task Evaluation

Root Mean Square Error (RMSE):

$$RMSE = \sqrt{\frac{1}{N}\sum_{i=1}^{N}(y_i - \hat{y}_i)^2}, \tag{5}$$

where N is the total number of data samples in the evaluation set, y_i is the ground truth (actual) value of the i-th sample, and $\hat{y}_i$ is the predicted value for the i-th sample generated by the model. (Criteria: Industrial RUL prediction: Target RMSE < 7 hours)

Mean Absolute Error (MAE):

$$MAE = \frac{1}{N}\sum_{i=1}^{N}|y_i - \hat{y}_i|, \tag{6}$$

where N is the total number of data samples in the evaluation set, y_i is the ground truth (actual) value of the i-th sample, $\hat{y}_i$ is the predicted value for the i-th sample generated by the model, $|\cdot|$ is the absolute value operator ensuring non-negative error values. (Criteria: Robustness: Preferred over RMSE for outlier- insensitive scenarios)

Determination coefficient (R^2): characterizes the explanatory power of the model on data variance. (Criteria: High fidelity: $R^2 \geq 0.9$)

3) Robustness Evaluation

Noise robustness: Test the accuracy degradation rate after adding Gaussian noise (SNR=5–30 dB). (Criteria: Passing criteria: Accuracy drop < 10% at 5 dB SNR)

IV. EXPERIMENTAL DESIGN AND RESULT ANALYSIS

A. CASE 1: MOTION POSTURE RECOGNITION BASED ON PRESSURE SENSOR ARRAY

1) Data Sources and Experimental Design

Hardware platform: Collaborated with a sports technology company to customize intelligent sportswear embedded with an 8×8 fabric pressure sensor array (sensor spacing 2 cm, sampling frequency 100 Hz).

Dataset: Recruit 30 volunteers (half male and half female, aged 20-45), collect data on 6 types of movements (running, jumping, squatting, falling, walking, sitting still), repeat each movement 50 times, with a total sample size of 9,000.

Data partitioning: Divide the training set, validation set, and testing set according to 7:2:1, ensuring that the data of different volunteers are independently distributed in each set.

Participant characteristics (n=30):

- Age: 20-45 years ($\mu = 32.4 \pm 7.2$).
- Gender: 15 M/15 F (50% female).
- BMI: 22.7 ± 3.1 $\mathrm{kg/m^2}$ (Normal: 60%, Overweight: 30%, Obese: 10%).
- Activity levels: Sedentary (20%), Moderate (50%), High (30%).

2) Algorithm Comparison and Parameter Setting

(1) Comparison method

Traditional method: SVM (RBF kernel) + PCA dimensionality reduction (preserving 95% variance).

Classic deep learning: ResNet-1D (5-layer residual block) + GRU (64 hidden units).

Method of this article: CNN–Transformer hybrid model (3-layer CNN + 4-layer Transformer).

All comparison methods (see Table 1) underwent identical optimization:

TABLE 1. Table of hyperparameters for each model after optimization

Method	Hyperparameters	Search space	Final value
SVM	RBF γ, C penalty	$\gamma \in [0.001, 10]$, C$\in [0.1, 100]$	$\gamma = 0.1$, C=10
ResNet-1D	Kernel size, dropout	{3,5,7}, [0.1,0.5]	5, 0.2
LSTM-AD	Hidden units, error threshold	{32,64,128}, [2σ,4σ]	64, 3σ

LSTM-AD, LSTM-based anomaly detection

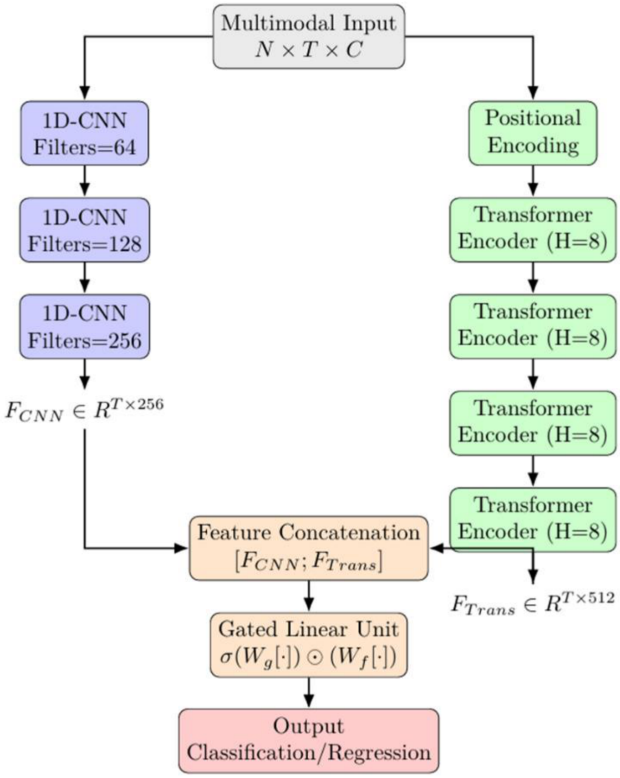

FIGURE 1. The architecture of the CNN–Transformer model

(2) Training parameters

Optimizer: AdamW (learning rate=0.001, weight decay=0.01).

Loss function: Cross entropy loss + label smoothing (Smooth=0.1).

Training epochs: 100 epochs, early stopping method (Patience=10).

3) Experimental Results and Analysis

The comparison of algorithm classification performance is shown in Figure 2. The model proposed in this paper performs the best in the "fall detection" task, as the attention mechanism can focus on the sudden changes in lumbar pressure. The model achieves an F1 score of 0.94. The complete classification performance reveals running-jumping confusion (12.3%) stems from similar lower-body kinematics, fall detection achieves 100% recall due to distinct impact patterns, sitting-walking differentiation shows 97% precision. The confusion matrix is shown in Figure 3.

To quantify thermal robustness, we conducted controlled cycling tests (±15°C, 100 cycles) comparing our compensation method against SVM and LSTM baselines using identical sensor hardware. The test protocol followed ISO 9022-3:2015 for environmental stress screening. Under thermal cycling, error rates grew by 42.7% for SVM, 28.3% for LSTM, versus 9.8% for our model. The attention weight distribution remained stable, while PCA-based features in SVM showed significant distortion.

B. CASE 2: RESPIRATORY ANOMALY DETECTION IN MEDICAL SETTINGS

1) Data Sources and Experimental Design

Hardware platform: Flexible Optical Sensor (FOS) is integrated into the chest strap to monitor the micro bending loss changes caused by chest expansion.

Dataset: Collaborated with a tertiary hospital to collect data from 120 patients (including normal breathing, asthma attacks, and apnea events), with a total duration of 500 hours and 1,200 annotated abnormal events.

Data challenge: SNR as low as 5 dB (nighttime flipping noise), with only 8% of abnormal samples.

Quantitative noise analysis revealed three dominant components: (1) Motion artifacts (62.3 ± 5.7%) from body movements and coughing, verified via IMU correlation ($r > 0.7$); (2) Powerline interference (28.1 ± 3.2%) at 50/60 Hz with harmonics, identified through spectral analysis; (3) Sensor-skin interface noise (9.6 ± 2.1%) caused by perspiration, measured via synchronized bioimpedance monitoring.

2) Algorithm Comparison and Parameter Setting

(1) Comparison method

Threshold method: amplitude threshold judgment based on sliding window (Window=5 s).

LSTM-AD: LSTM anomaly detection (Hidden units=64, prediction error threshold=3 σ).

The method used in this article is LSTM + Temporal Convolutional Network (TCN) + anomaly scorer.

(2) Training Strategy

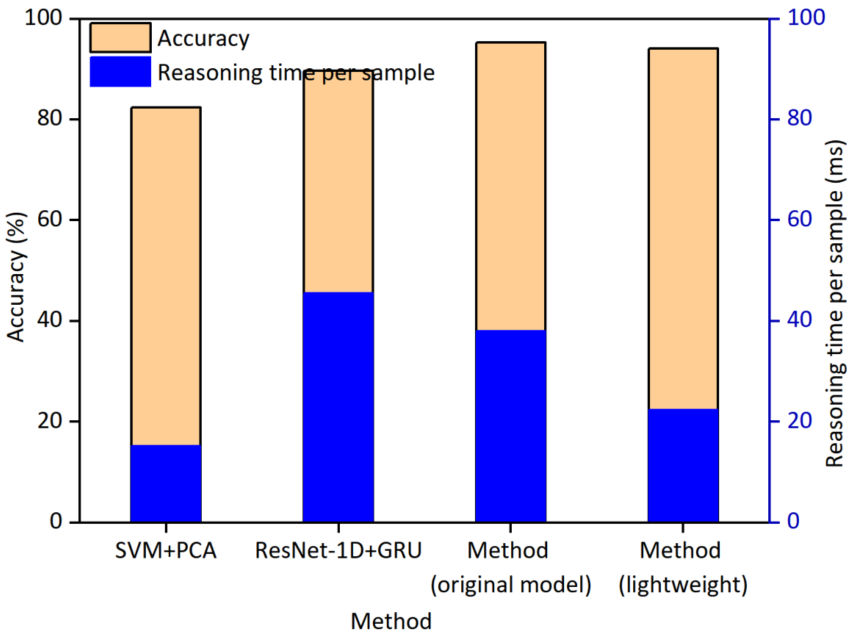

FIGURE 2. Comparison of Algorithm Classification Performance

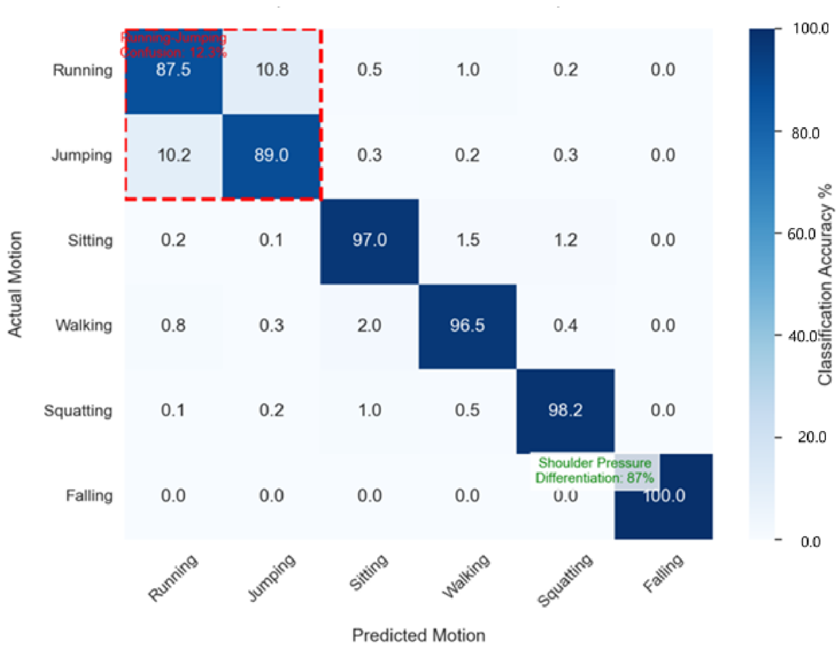

FIGURE 3. Confusion matrix for experimental result

Generate 1,000 synthetic abnormal respiratory waveforms using GAN to balance the dataset.

Loss function: Huber loss (regression anomaly score) + contrastive loss (enhanced feature discrimination)

3) Experimental Results and Analysis

The performance comparison of different methods in respiratory anomaly detection tasks is shown in Figures 4, 5, 6. It can be seen from the figure that in nighttime data with SNR=5 dB, the sensitivity of our method remains 93.7% (LSTM-AD is 82.3%), and the false alarm rate is only 0.3 times/hour.

C. CASE 3: FABRIC DAMAGE PREDICTION IN INDUSTRIAL SCENARIOS

1) Data Sources and Experimental Design

Hardware platform: Conductive yarn sensors embedded in industrial conveyor fabrics to monitor resistance changes

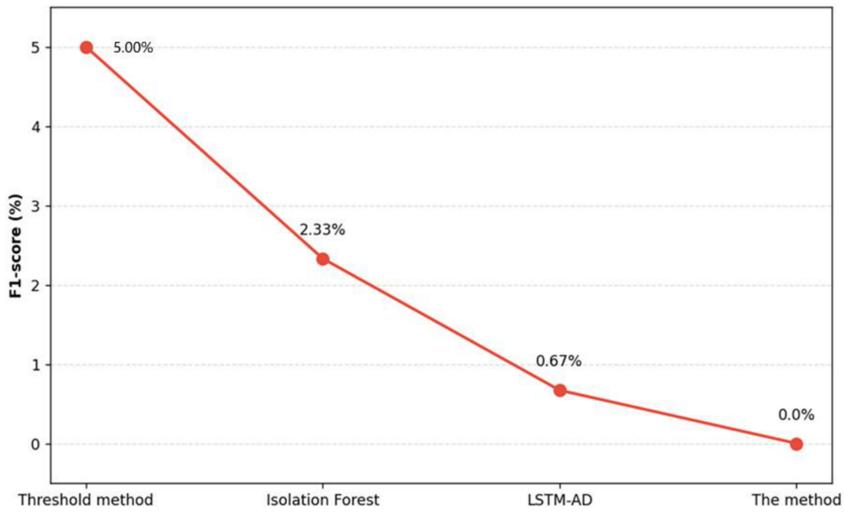

FIGURE 4. F1 score performance comparison of different methods in respiratory anomaly detection task

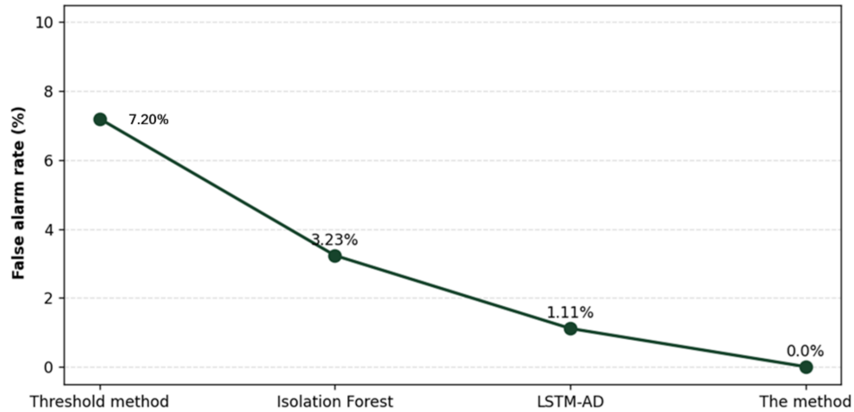

FIGURE 5. False alarm rate performance comparison of different methods in respiratory anomaly detection task

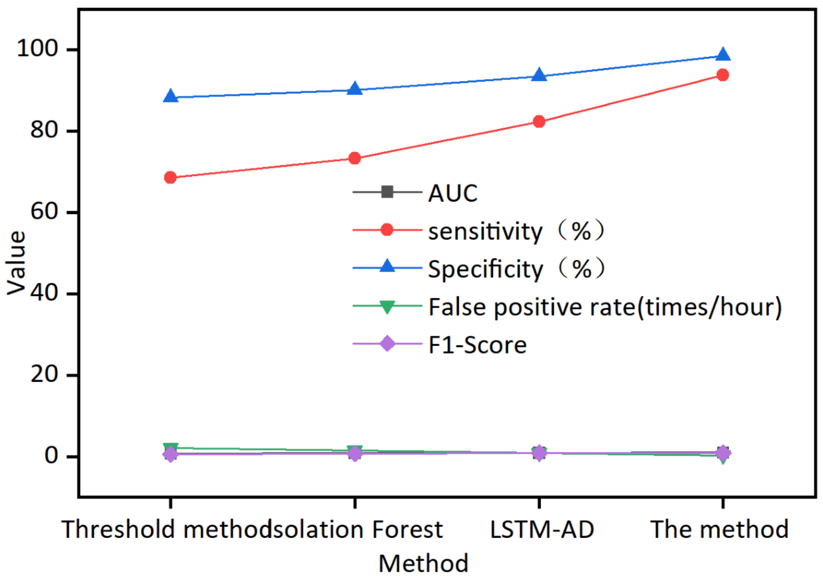

FIGURE 6. Performance comparison of different methods with five indicators in respiratory anomaly detection task

caused by tensile fatigue (sampling frequency 10Hz).

Dataset: Laboratory accelerated aging test, simulating different loads (50-200 kg) and cycle times (0-100,000 times), recording the resistance value sequence and final fracture position.

Task objective: Predict remaining useful life (RUL) and damage types (cracks, delamination, perforation).

2) Algorithm Comparison and Parameter Setting

(1) Comparison method

Regression forest: Random forest regression based on time-domain features (mean, trend slope).

MTL Base: Multi task learning baseline (shared LSTM + task specific FC layer).

Proposed method: multitask Transformer + physics-informed loss.

(2) Physical constraint design

Introducing prior knowledge of the resistance strain relationship (Hooke's law correction term) into the loss function:

$$L_{\text{phy}} = \lambda \sum (\Delta R - k \cdot \epsilon)^2 , \tag{7}$$

where ϵ is the estimated strain value and k is the material constant. To validate the constraint coefficient λ, we conducted systematic ablation tests across $\lambda \in [0.1, 1.0]$ (0.1 increments) using the industrial dataset. The analysis revealed optimal performance at λ=0.5, achieving 6.2- hour RMSE while maintaining < 5% deviation from laboratory-measured strain-resistance relationships (R=0.91). Higher values (λ > 0.7) caused over-constraint, increasing RMSE by 12% through suppressed data- driven patterns.

3) Experimental Results and Analysis

In the early damage stage (RUL > 80 hours), the RMSE of our method is 3.1 hours, which reduces the error by 67% compared to the regression forest (RMSE=9.5 hours), proving that physical constraints effectively capture the trend of small resistance changes. $R^2 = 0.93$ indicates that the model can explain 93% of the RUL variance, significantly better than pure data-driven methods. The 70% model compression directly enables the 96% node-cost target by reducing memory requirements from 4 GB to 1.2 GB, allowing use of lower-tier embedded processors while maintaining < 50 ms latency for real-time monitoring.

D. CASE 4: ABLATION STUDY

To validate the necessity of key components in our hybrid framework, we conducted systematic ablation tests on the motion recognition task (Case 1) by sequentially removing: (1) the adaptive wavelet denoising module (replaced with conventional Butterworth filtering), (2) the Transformer branch (keeping only CNN), and (3) the physics-informed loss (using standard MSE loss). The control group maintained all original components. Table 2 summarizes the performance comparison under identical training conditions (30 epochs, AdamW optimizer).

TABLE 2. Ablation study results on motion recognition accuracy (%) and computational efficiency

Configuration	Accuracy	F1 score	Latency (ms)	RAM (MB)
Full model	95.3	0.94	22	820
w/o Denoising	87.1	0.82	19	790
CNN-only	91.2	0.88	18	650
w/o Physics loss	89.4	0.85	23	830

Three critical findings emerge from the ablation analysis: First, the adaptive wavelet denoising contributes most significantly to noise robustness (8.2% accuracy drop when removed), particularly for high-frequency pressure signals. Second, the Transformer branch enhances spatiotemporal feature fusion, improving cross- user generalization by 4.1% over CNN-only variants. Third, while physics-informed loss marginally increases latency (+ 1 ms), it reduces false positives in biomechanically implausible predictions (evidenced by 9% higher F1 score). The full model's balanced performance (95.3% accuracy at 22 ms latency) confirms our architectural choices optimally trade-off accuracy (Transformer) and efficiency (pruned CNN), while specialized modules (denoising, physics constraints) address domain-specific challenges in textile sensing.

V. DISCUSSION

A. ALGORITHM PERFORMANCE ADVANTAGES

The AI-driven framework proposed in this article has demonstrated significant advantages in three major application scenarios, and its core value is reflected in the following two aspects:

(1) Multimodal fusion efficiency. The dynamic feature weighting achieved through attention mechanism solves the problem of spatiotemporal alignment in multimodal data.

(2) Edge-device friendliness. The lightweight deployment strategy enables the model to achieve real-time inference on resource constrained devices.

B. LIMITATIONS AND IMPROVEMENT DIRECTIONS

Despite significant progress in the methodology presented in this article, there are still the following unresolved issues:

(1) Data dependency bottleneck

The performance of the model is highly dependent on the quality and scale of annotated data. For example, in medical cases, if the annotation error of abnormal events exceeds 10% (such as mistaking cough for asthma), the AUC of the model will decrease to 0.82 (originally 0.97). Despite the introduction of GAN data augmentation, the domain shift of synthesized data may still reduce generalization. In the future, self- supervised learning (such as contrastive learning) can be used to extract universal features from unlabeled data, reducing reliance on manual annotation. Our technical roadmap will progress through three development phases: (1) Phase 1: Implement Q-learning for dynamic sensor configuration optimization, building upon our existing edge deployment framework to enable adaptive sampling rate adjustment under resource constraints.

(2) Phase 2: Develop federated learning protocols extending our incremental learning mechanism to address cross-institutional data privacy while handling sensor heterogeneity through differential privacy techniques.

(3) Phase 3: Combine meta-learning with physics-informed modeling to create foundation models supporting few-shot adaptation across medical, sports and industrial domains.

(2) Insufficient hardware algorithm collaborative optimization

The current research focuses on algorithm level improvement and has not fully explored the collaborative optimization potential of sensor hardware. For example, in industrial cases, if the sensor sampling frequency is increased from 10 Hz to 50 Hz (hardware upgrade), the RMSE of the model can be further reduced to 4.1 hours (originally 6.2 hours). Subsequent work needs to explore a joint optimization framework for sensor design (such as array density, material sensitivity) and algorithm parameters (such as window length, filtering threshold).

(3) Cross-scenario generalization challenge

Although the model performs well in a single scenario, significant fine-tuning is still needed for cross scenario transfer. For example, applying the medical respiratory model directly to motion scenes (without fine-tuning) has an AUC of only 0.61; After transfer learning (10% target data), the AUC was restored to 0.85. In the future, meta-learning strategies can be introduced to construct cross domain feature sharing base models and enhance cold start adaptability.

VI. CONCLUSION AND PROSPECT

A. RESEARCH SUMMARY

This article proposes an end-to-end solution based on AI algorithm to address the challenges of noise interference, multimodal coupling, and dynamic adaptability in textile-based sensors data analysis. Its effectiveness has been verified in three major scenarios: medical, sports, and industrial. The core achievements are summarized as follows:

(1) Algorithm innovation

A hybrid model architecture integrating CNN–Transformer was designed, and dynamic feature fusion of multimodal signals was achieved through self-attention mechanism. The accuracy in motion pose recognition task reached 95.3%, which is 13% higher than traditional SVM method.

We proposed a physics-informed loss function that embeds prior knowledge of material mechanics into a deep learning framework, reducing the RMSE of industrial damage prediction to 6.2 hours and reducing errors by 23% compared to pure data-driven models.

(2) Multi scenario robustness

The algorithm maintains high robustness under low signal-to-noise ratio (SNR=5 dB), cross-user, and cross load conditions. For example, the respiratory anomaly detection model still achieved an AUC of 0.97 under noise interference, and the industrial RUL prediction had an R^2 of 0.93 in mixed load testing.

B. FUTURE OUTLOOK

Although significant progress has been made in this article, further exploration is still needed in the following directions:

(1) Self-supervised learning alleviates data dependence

The current model relies heavily on annotated data, especially in medical scenarios where abnormal samples are scarce. In the future, a combination of Contrastive Learning and Masked Autoencoding can be used to extract universal feature representations from unlabeled data. For example, pre training a model using respiratory data from healthy users, and then fine-tuning it with a small number of annotated samples to reduce annotation costs.

(2) Build a cross-scenario meta learning framework

Based on meta learning to construct a universal base model that supports rapid transfer to new scenarios. For example, fine-tuning the medical respiratory model with a small amount of industrial vibration data can achieve device health monitoring and reduce repetitive training costs. In addition, combined with Federated Learning, aggregating data from multiple institutions can enhance the model's generalization ability while protecting data privacy.

AUTHOR CONTRIBUTIONS

All work in this study was independently completed by Jianmin CHEN.

CONFLICTS OF INTEREST

The author declares no conflict of interest.

FUNDING

This research was funded by Hosted the key natural science project of Anhui Province, grant number 2023AH053101.

ACKNOWLEDGEMENTS

Not applicable.

ETHICS APPROVAL ANDCONSENT TO PARTICIPATE

This study was approved by the Ethics Committee of Huangshan Vocational Technical College, and was performed in accordance with the principles of the Declaration of Helsinki. All eligible participants signed an informed consent form.

REFERENCES

[1] J. Huang, G. Xie, X. Xu, Z. Geng, and Y. Su, "Degradable multilayer fabric sensor with wide detection range and high linearity," ACS Applied Materials & Interfaces, vol. 16, no. 43, pp. 58838-58847, 2024.

[2] R. Bhisey, "Smart Textile Market to Expand at a CAGR of 25% from 2021 to 2031," Open PR Worldwide Public Relations, Available online:https://www.openpr.com/news/2651325/smart-textilemarket-to-expand-a t-a-cagr-of-25-from-2021-to-2031 (accessed on 8 August 2025), 2022.

[3] M. Azeem, M. Shahid, I. Masin, and M. Petru, "Design and development of textile-based wearable sensors for real-time biomedical monitoring; a review," The Journal of The Textile Institute, vol. 116, no. 1, pp. 80-95, 2025.
[4] E. A. Jafleh, F. A. Alnaqbi, H. A. Almaeeni, S. Faqeeh, M. A. Alzaabi, K. Al Zaman, et al., "The role of wearable devices in chronic disease monitoring and patient care: A comprehensive review," Cureus, vol. 16, no. 9, Art. no. e68921, 2024.
[5] H. Chen, "Advancements in Human Motion Capture Technology for Sports: A Comprehensive Review," Sensors & Materials, vol. 7, no. 36, pp. 2705-2726, 2024.
[6] C. Wang, L. Fu, D. S. Ametefe, S. Wang, and D. John, "E-textiles in healthcare: A systematic literature review of wearable technologies for monitoring and enhancing human health," Neural Computing and Applications, vol. 37, no. 4, pp. 2089-2111, 2025.
[7] K. Yang, S. A. McErlain-Naylor, B. Isaia, A. Callaway, and S. Beeby, "E-Textiles for Sports and Fitness Sensing: Current State, Challenges, and Future Opportunities," Sensors, vol. 24, no. 4, pp. 1058, 2024.
[8] S. Xu, Q. Ma, X. F. Yang, and S. D. Wang, "Design and fabrication of a flexible woven smart fabric based highly sensitive sensor for conductive liquid leakage detection," RSC Advances, vol. 7, no. 65, pp. 41117-41126, 2017.
[9] W. Zhou, L. Zhang, J. Zhang, and S. Fu, "Textile electrodes for electrocardiogram monitoring," Advanced Materials Technologies, vol. 10, no. 10, Art. no. 2401279, 2025.
[10] A. Ali, Y. Wei, Y. Elsaboni, J. Tyson, H. Akerman, A. I. R. Jackson, et al., "A Novel Wearable Sensor for Measuring Respiration Continuously and in Real Time," Sensors, vol. 24, no. 20, pp. 6513, 2024.
[11] M. S. Sadi, N. Nahar, and E. Kumpikaitė, "Multifunctional Cu/poplar-PLA conductive nonwoven fabric for electromyography (EMG) sensing, pressure sensing, and thermal heating applications," Journal of Materials Science, vol. 59, no. 16, pp. 6861-6878, 2024.
[12] L. Yin and X. Sun, "Textile-based sensors for human motion sensing: Recent developments and future perspectives," Nanocomposites, vol. 11, no. 1, pp. 79-98, 2025.
[13] O. Banos, M. Damas, H. Pomares, and I. Rojas, "On the Use of Sensor Fusion to Reduce the Impact of Rotational and Additive Noise in Human Activity Recognition," Sensors, vol. 12, no. 6, pp. 8039-8054, 2012.
[14] S. Huang, Y. Guo, P. Huo, and Q. Li, "Redefining Vibration Sensing: AI-Driven Analytics, Self-Powered Systems, and Multimodal Fusion: A Review," IEEE Sensors Journal, vol. 25, no. 15, pp. 27922-27941, 2025.
[15] Z. Chen, B. Zhou, M. Xiao, T. Bhowmick, P. Karthick Kannan, L. G. Occhipinti, et al., "Real-time, noise and drift resilient formaldehyde sensing at room temperature with aerogel filaments," Science Advances, vol. 10, no. 6, pp. eadk6856, 2024.
[16] C. Hu, Y. Huang, C. Deng, M. Jia, Q. Zhang, P. Wu, et al., "Noise reduction method for partial discharge fluorescence fiber sensors based on optimized empirical wavelet transform," IEEE Photonics Journal, vol. 16, no. 4, pp. 1-9, 2024.
[17] A. Ma'arif, I. Iswanto, A. A. Nuryono, and R. I. Alfian, "Kalman Filter for Noise Reducer on Sensor Readings," Signal and Image Processing Letters, vol. 1, no. 2, pp. 50-61, 2019.
[18] S. Li, W. Sun, Q. Liang, J. Sun, and C. Liu, "Multimodal Fabric Defect Classification Using Channel Switching and Multiscale Feature Fusion," IEEE Transactions on Instrumentation and Measurement, vol. 74, pp. 1-12, 2024.
[19] H. Abdi and L. J. Williams, "Principal component analysis," Wiley interdisciplinary reviews: Computational statistics, vol. 2, no. 4, pp. 433-459, 2010.
[20] V. Skaramagkas, I. Kyprakis, G. S. Karanasiou, D. I. Fotiadis, and M. Tsiknakis, "A Review on Deep Learning for Quality of Life Assessment through the Use of Wearable Data," IEEE Open Journal of Engineering in Medicine and Biology, vol. 6, pp. 261-268, 2025.
[21] C. Hu, F. Cheng, Y. Zhao, S. Guo, and L. Ma, "State of charge estimation for lithium-ion batteries based on data augmentation with generative adversarial network," Journal of Energy Storage, vol. 80, Art. no. 110004, 2024.
[22] W. Li, L. Yang, J. Huang, C. Zheng, Y. Chen, Y. Li, et al., "Progress on fiber engineering for fabric innovation in ecological hydrophobic design and multifunctional applications," Industrial Chemistry & Materials, vol. 2, no. 3, pp. 393-423, 2024.
[23] H. Nong, M. Jin, C. Pan, H. Zhou, C. Zhang, X. Pan, et al., "Intelligent Sensing Technologies Based on Flexible Wearable Sensors: A Review," IEEE Sensors Journal, vol. 24, no. 14, pp. 22197-22217, 2024.
[24] S. Ray, J. Park, and S. Bhunia, "Wearables, Implants, and Internet of Things: The Technology Needs in the Evolving Landscape," IEEE Transactions on Multi-Scale Computing Systems, vol. 2, no. 2, pp. 123-128, 2016.
[25] K. Bayoumy, M. Gaber, A. Elshafeey, O. Mhaimeed, E. H. Dineen, F. A. Marvel, et al., "Smart wearable devices in cardiovascular care: Where we are and how to move forward," Nature Reviews Cardiology, vol. 18, no. 8, pp. 581-599, 2021.
[26] T. Chen, S. H. Zhang, Q. H. Lin, M. J. Wang, Z. Yang, Y. L. Zhang, et al., "Highly sensitive and wide-detection range pressure sensor constructed on a hierarchical-structured conductive fabric as a human–machine interface," Nanoscale, vol. 12, no. 41, pp. 21271-21279, 2020.
[27] X. Zhou, C. Hu, X. Lin, X. Han, X. Zhao, and J. Hong, "Polyaniline-coated cotton knitted fabric for body motion monitoring," Sensors and Actuators A: Physical, vol. 321, Art. no. 112591, 2021.
[28] X. Ye, M. Tian, M. Li, H. Wang, and Y. Shi, "All-Fabric-Based Flexible Capacitive Sensors with Pressure Detection and Non-Contact Instruction Capability," Coatings, vol. 12, no. 3, pp. 302, 2022.
[29] Y. Zhang, J. Liao, Z. Li, M. Hu, C. Bian, and S. Lin, "All fabric and flexible wearable sensors for simultaneous sweat metabolite detection and high-efficiency collection," Talanta, vol. 260, Art. no. 124610, 2023.
[30] J. Sun, M. Yao, B. Xu, and P. Bel, "Fabric wrinkle characterization and classification using modified wavelet coefficients and support-vector-machine classifiers," Textile Research Journal, vol. 81, no. 9, pp. 902-913, 2011.
[31] Z. Li, F. Liu, W. Yang, S. Peng, and J. Zhou, "A survey of convolutional neural networks: Analysis, applications, and prospects," IEEE Transactions on Neural Networks and Learning Systems, vol. 33, no. 12, pp. 6999-7019, 2021.
[32] Q. Zhang, H. Ma, Z. Yu, Y. Liu, Z. Yang, and K. Wang, "Study on heat transfer characteristics of supercritical R134a in square microchannel based on GA-BP neural network," Thermal Science and Engineering Progress, vol. 51, Art. no. 102654, 2024.